

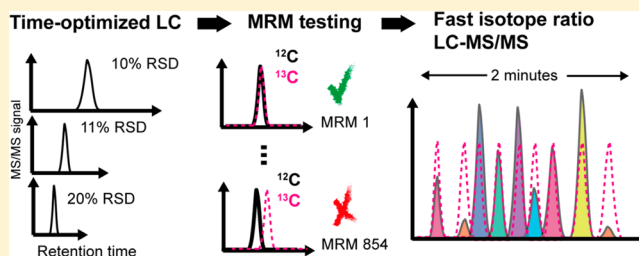
Time-Optimized Isotope Ratio LC–MS/MS for High-Throughput Quantification of Primary Metabolites

Jan Christopher Guder, Thorben Schramm, Timur Sander, and Hannes Link*

Max Planck Institute for Terrestrial Microbiology, Karl-von-Frisch-Strasse 16, 35043 Marburg, Germany

 Supporting Information

ABSTRACT: Cellular metabolite concentrations hold information on the function and regulation of metabolic networks. However, current methods to measure metabolites are either low-throughput or not quantitative. Here we optimized conditions for liquid chromatography coupled to tandem mass spectrometry (LC–MS/MS) for quantitative measurements of primary metabolites in 2 min runs. In addition, we tested hundreds of multiple reaction monitoring (MRM) assays for isotope ratio mass spectrometry of most metabolites in amino acid, nucleotide, cofactor, and central metabolism. To systematically score the quality of LC–MS/MS data, we used the correlation between signals in the ^{12}C and ^{13}C channel of a metabolite. Applying two optimized LC methods to bacterial cell extracts detected more than 200 metabolites with less than 20% variation between replicates. An exhaustive spike-in experiment with 79 metabolite standards demonstrated the high selectivity of the methods and revealed a few confounding effects such as in-source fragments. Generally, the methods are suited for samples that contain metabolites at final concentrations between 1 nM and 10 μM , and they are sufficiently robust to analyze samples with a high salt content.



The ability to measure many metabolites in hundreds of samples per day is essential for large-scale investigations of metabolic networks. Current high-throughput metabolomics methods detect many metabolites within minutes or seconds using direct or flow injection mass spectrometry.^{1–4} These untargeted methods have the disadvantages that they are not quantitative and identification of metabolites can be ambiguous.⁵ Yet, absolute quantitation of selected metabolites plays an important role in hypothesis-driven studies,⁶ metabolic engineering approaches,⁷ and the development of metabolic models.⁸ For this purpose, targeted metabolomics methods were developed that use fragmentation and chromatography to achieve high selectivity and specificity. In addition to gas chromatography and capillary electrophoresis, liquid chromatography coupled to mass spectrometry (LC–MS/MS) is a key technology for targeted metabolomics.^{9–11} Highest quantitative accuracy is achieved by spiking samples with isotopically labeled internal standards to correct matrix effects, drifts of mass spectrometers, and losses during sample preparation.^{12,13} Moreover, comparing chromatography peaks of labeled and unlabeled metabolites is essential to unequivocally identify metabolites and avoid misannotation.¹⁴ Isotopically labeled internal standards for primary metabolites are easily obtained from cell extracts of yeast or bacteria that were cultivated on uniformly ^{13}C labeled glucose as the sole carbon source. These cell extracts are then added to the biological sample (ideally during the extraction step), and the ratio of unlabeled and labeled metabolites is determined by LC–MS/MS.

For LC–MS/MS, either triple quadrupole mass spectrometers (QqQ) operated in multiple reaction monitoring (MRM)

mode or high-resolution mass spectrometers are frequently applied. Especially QqQ instruments are capable of very fast and sensitive MRM assays and allow effective polarity switching.⁵ However, despite the improved speed and sensitivity of up-to-date mass spectrometers, current LC–MS/MS based metabolomics methods have still long instrument cycle times to achieve sufficient chromatographic separation. Consequently, the first important step toward quantitative high-throughput metabolomics is the development of time-optimized LC. Different conditions are currently used for LC separation of the mostly polar metabolites in primary metabolism. For example, reversed-phased ion-pairing methods are capable to separate a very large spectrum of metabolites including isomers.^{9,11} Unfortunately, ion-pairing reagents reduce sensitivity of mass spectrometers and cause ion suppression. Methods that are more compatible with mass spectrometry include hydrophilic interaction liquid chromatography (HILIC) and aqueous normal phase (ANP) chromatography using stationary phases of unmodified or derivatized silica.^{10,15,16} Recent improvements of ANP and HILIC methods include diamond hydride-based columns¹⁷ and zwitterionic materials.¹⁸ Further, ultrahigh-performance LC with smaller particles and smaller columns can increase peak capacity and enable very fast separations.^{19,20} However, the fastest LC–MS/

Received: September 21, 2016

Accepted: January 2, 2017

Published: January 3, 2017

Table 1. Conditions and Reproducibility of 24 Fast LC Methods^a

Column	Acquity BEH Amide								iHILIC-Fusion(P)								Zorbax				D. Hydride							
Dimension	30 x 2.1 mm								50 x 2.1 mm								30 x 2.1 mm				30 x 2.1 mm							
Particle size	1.7 μm								5 μm								1.8 μm				2.2 μm							
pH	acidic				basic				acidic				basic				acidic				acidic							
Run time (min)	3.8	2.5	2	1.5	3.8	2.5	2	1.5	3.8	2.5	2	1.5	3.8	2.5	2	1.5	3.8	2.5	2	1.5	3.8	2.5	2	1.5	3.8	2.5	2	1.5
Flow rate (mL min ⁻¹)	0.2	0.3	0.4	0.5	0.2	0.3	0.4	0.5	0.2	0.3	0.4	0.5	0.2	0.3	0.4	0.5	0.2	0.3	0.4	0.5	0.2	0.3	0.4	0.5	0.2	0.3	0.4	0.5
Median RSD	10	9	12	19	11	11	11	11	10	12	12	14	8	10	10	14	11	11	12	13	12	10	13	14	12	10	13	14
#of metabolites RSD<20%	27	26	25	14	34	30	29	23	11	15	23	19	26	31	34	27	23	27	24	24	25	25	22	21	25	25	22	21

^aMethods A and B are indicated in gray.

MS based metabolomics methods still rely on measurement times of more than 10 min.^{21,22}

Here we established LC methods with short columns coupled to a fast and sensitive QqQ instrument in order to quantify primary metabolites in 2 min runs. First, we optimized LC conditions in HILIC and ANP mode in order to achieve fast and reproducible measurements of central metabolites, as well as compounds in amino acid, nucleotide, and cofactor metabolism. The two best LC methods with acidic and basic mobile phase were used to test MRM assays for 419 metabolites. These data were systematically scored based on the correlation between ¹²C and ¹³C chromatograms, which allowed detecting 233 high-scoring metabolites in *E. coli* cell extracts. We validated the fast LC–MS/MS methods by spiking samples with 79 authentic standards and by repetitive measurements of the same sample. All samples were non-concentrated metabolite extracts from *Escherichia coli* cultures in a mixture of acetonitrile/methanol/water (40:40:20).¹² In order to apply the methods to other samples they should contain a similar amount of organic solvent and metabolites at final concentrations between 1 nM and 10 μM.

EXPERIMENTAL SECTION

Chemicals and Materials. LC eluents were water from an ultrapure water system (ELGA LabWater) and acetonitrile LC–MS Ultra Chromasolv (Sigma-Aldrich). LC additives were ammonium hydroxide TraceSELECT Ultra (Fluka Analytical), formic acid for LC–MS (Fluka Analytical), ammonium formate >99% for LC–MS (Fluka Analytical), and ammonium carbonate 99.999% (Sigma-Aldrich). The four LC columns were Hilic Plus ZORBAX (Agilent Technologies), Acquity UPLC BEH Amide (Waters), Cogent Diamond Hydride (MicroSolv), and iHILIC-Fusion(P) (HILICON AB). Column dimensions and particle sizes are listed in Table 1. U-¹³C glucose (99%) was obtained from Cambridge Isotope Laboratories.

Metabolite Standards. Authentic metabolite standards were obtained from Sigma-Aldrich. Stock solutions of metabolites were prepared by dissolving standards in water. From stock solutions, a 10 μM standard mixture was prepared in 50:50 (v/v) methanol/water with 10 mM ammonium acetate at pH 7. Aliquots of the mixture were stored at –80 °C. Parameters for MRM assays in positive and negative ionization mode were determined using flow injection of single standards

at a concentration of 1 μM. For spike-in experiments, we added standards individually to metabolite extracts at a final concentration of 1 μM.

Bacterial Cultures and Sampling. *E. coli* MG1655 (DSMZ No. 18039) was cultured in 500 mL shake flasks at 37 °C in 30 mL of M9 minimal medium containing 5 g L⁻¹ glucose. Cells were grown to an optical density at 600 nm (OD) between 0.8 and 1. In the culture treated with trimethoprim, the drug was added at the same OD to a final concentration of 10 μg mL⁻¹, and the sample was collected after 30 min. For sampling of metabolites by filtration, 2 mL culture aliquots were vacuum-filtered on a 0.45 μm pore size filter (HVLP02500, Merck Millipore), and filters were immediately transferred into 40:40:20 (v-%) acetonitrile/methanol/water with ¹³C internal standard kept at –20 °C. For sampling of the whole cell broth, 1 mL of culture was transferred into 4 mL of 50:50% acetonitrile/methanol in a 15 mL Falcon tube cooled to –20 °C. Extracts were centrifuged for 15 min at 13 000 rpm at –9 °C, and the supernatant was directly used for LC–MS/MS.

Preparation of ¹³C Internal Standard. *E. coli* MG1655 (DSMZ No. 18039) was grown in 100 mL of M9 minimal medium containing 4 g L⁻¹ uniformly ¹³C-labeled glucose (Cambridge Isotope Laboratories) to an OD of 1. The culture broth was aerated using air passed through 4 M potassium hydroxide in order to avoid incorporation of ¹²C by CO₂. Aliquots of 20 mL were vacuum-filtered using 0.45 μm pore size filters (HVLP02500, Merck Millipore) and immediately transferred into 5 mL of 40:40:20 (v-%) acetonitrile/methanol/water kept at –20 °C. Half of the culture was treated with a mixture of ampicillin, chloramphenicol, rifampicin, and trimethoprim for 15 min before sampling. Final extracts from glucose-grown cells and inhibitor treated cells were mixed 1:1, and aliquots were stored at –80 °C.

Liquid Chromatography. An Agilent 1290 Infinity II UHPLC system (Agilent Technologies) was used for liquid chromatography. Temperature of the column oven was 30 °C. A 0.3 μm inline filter was used (Agilent Technologies) and no guard column. LC solvents were kept in Teflon FEP bottles (Nalgene, Thermo Scientific) with PTFE inlet filters (Vici Jour). The injection volume for all methods was 3 μL. LC solvents A were water with 10 mM ammonium formate and 0.1% formic acid (v/v) for acidic conditions and water with 10 mM ammonium carbonate and 0.2% ammonium hydroxide for

basic conditions. LC solvents B were acetonitrile with 0.1% formic acid (v/v) for acidic conditions and acetonitrile without additive for basic conditions. The gradients were: 0 min 90% B; 0.5/X min 40% B; 0.6/X min 40% B; 0.65/X min 90% B; 0.75/X min 90% B, where X is the flow rate as given in Table 1. The time between injections was 0.5 min.

Mass Spectrometry. An Agilent 6495 triple quadrupole mass spectrometer (Agilent Technologies) was used for mass spectrometry. Source gas temperature was set to 200 °C, with 14 L min⁻¹ drying gas and a nebulizer pressure of 24 psi. Sheath gas temperature was set to 300 °C and flow to 11 L min⁻¹. Electrospray nozzle and capillary voltages were set to 500 and 2500 V, respectively. Dwell times of 8 ms were used for MRM assays of 40 metabolites for the initial testing of LC conditions. Groups of 40 MRMs with dwell times of 20 ms were used to tests the 854 MRM parameters that are listed in Table S2.

Data Analysis. Data processing and analysis was performed with Matlab R2014b. LC-MS/MS raw data were converted using MSconvert.²³ Selection of peaks of metabolite *i* in *j* = *N* samples was as follows: (1) peaks with a prominence >0.1 were selected in the ¹²C and ¹³C channel of metabolite *i*. (2) If ¹²C and ¹³C maxima lay 5 data points next to each other, these peak pairs were retained. (3) The correlation of all peak pairs was determined using 11 data points around the maximum of the ¹²C peak, and the highest correlating peak pair was selected. After peaks were selected for sample 1 to *N*, the retention time occurring most often in all samples was determined as $RT_i = \text{mode}(RT_{ij})$, where $j = 1 - N$. This ensured that the same peak pairs were selected for all samples. Subsequently the ¹²C peak and ¹³C peak next to RT_i were selected in all samples and the correlation was again determined as described above. The algorithm is given in Matlab format in the Supporting Information. The Pearson correlation was used in all cases, and unless stated otherwise a value of 0.8 was the cutoff for high-scoring chromatograms. Quantification of intracellular metabolite concentrations was based on the ratio of ¹²C and ¹³C peak heights as described previously.¹² A specific cell volume of 2 μL mg(dry weight)⁻¹ was used to calculate the cell volume.

RESULTS AND DISCUSSION

Time-Optimized LC of Primary Metabolites. In order to identify suitable conditions for fast LC of primary metabolites, we tested the separation of 40 metabolites that we selected based on their chemical diversity. For example, six nucleotides represented pyrimidine and purine nucleotide mono-, di-, and triphosphates. Nine amino acids represented aliphatic, aromatic, acidic, basic, hydroxylic, amidic, and sulfur-containing amino acids. In total, 12 compounds were from central metabolic pathways (e.g., sugar phosphates, Acetyl-CoA) and 4 were cofactors (Table S1). In total 24 LC methods were tested. These methods were based on 4 short LC columns, using acidic and basic mobile phase, and 4 flow rates with gradients between 4 and 1.5 min (Table 1). A standard solution containing 1 μM of the 40 metabolites was spiked with ¹³C internal standard (¹³C-IS) and measured 6 times with each method. To test for carry-over, we injected blanks between two measurements. Reproducibility of the methods was calculated as the relative standard deviation (RSD) of the ratio of ¹²C and ¹³C peak heights for each metabolite. In general, the quality of separation of each metabolite depended on the combination of stationary and mobile phase. Therefore, we scored the

measurements based on the correlation between signals in the ¹²C and ¹³C channel of a metabolite and only retained high-scoring chromatograms (Experimental Section). Reduced measurement time resulted only in a slight increase of the median RSD (Table 1 and Table S1).

All methods except the fast 1.5 min methods had median RSDs between 8% and 13%, which is comparable to existing methods using longer chromatography.^{9,10} The 1.5 min methods had higher RSDs between 11% and 19%. The best result was obtained with the 50 mm iHILIC column using basic mobile phase in the 2 min run. This method showed a median RSD of 10% and separated 34 metabolites with an RSD < 20%. With acidic mobile phase the Acquity, Zorbax, and Diamond Hydride column performed almost equally well. We selected the Acquity column and a 2 min gradient, which separated most metabolites under this condition and showed a median RSD of 12%. The pH of the mobile phase had a large effect on peak shapes and separation of metabolites, e.g., nucleotide triphosphates only separated with basic mobile phase, and best peak shapes were achieved in combination with the iHILIC column (Figure 1). Most amino acids on the other hand separated best with acidic mobile phase (Figure 1). Based on these results we decided to further optimize the 2 min runs with the Acquity column and acidic mobile phase (Method A) and the iHILIC column with basic mobile phase (Method B).

MRM Assays for Detection of 419 Metabolites. To increase coverage of metabolites by fast LC-MS/MS, we collected parameters for MRM assays of 419 metabolites in their labeled and unlabeled form. MRM parameters were either determined by single compound optimization or obtained from the literature.⁹⁻¹¹ For metabolites where no standards or literature information was available, we obtained predicted MRMs from the CFM-ID Web server.²⁴ The tested metabolites included 54 compounds of central metabolism, 138 of amino acid metabolism, 86 of nucleotide metabolism, and 116 in cofactor metabolism. In total, 25 metabolites were precursors of lipid and membrane biosynthesis and other compounds. Where possible, we collected multiple MRM parameters for each metabolite in positive and negative ionization mode resulting in 1708 MRM assays (Table S2). We then went on to systematically test MRMs in groups of 40 with the 2 min LC-MS/MS Methods A and B. To this end, we prepared a fresh ¹²C cell extract in the same way as the ¹³C-IS, which was obtained from a batch culture of glucose-grown *E. coli*. Half of the culture was directly extracted, and the other half was treated with a mixture of inhibitors before extraction, in order to increase the concentration of low-abundance metabolites (Experimental Section). The ¹²C and ¹³C cell extracts were mixed and measured three times with each method. Subsequently, we evaluated the measurements based on the RSD of the three replicates and the ¹²C/¹³C correlation score (Table S2). For those metabolites with multiple MRMs, we selected the highest scoring one. Out of all 419 metabolites tested, 233 had a score >0.8 and an RSD < 20% (Figure 2). These included all 20 amino acids except cysteine and all purine and pyrimidine nucleotide mono-, di-, and triphosphates except GDP. Notably, the fraction of metabolites with low RSDs increased with higher scores (Figure 2). We also inspected the differences between ¹²C/¹³C ratios determined with both methods. When measurements with both methods had a correlation based score >0.8, the median difference was lower than 20%. Measurements with higher score had smaller differences and vice versa (Figure S1). Out of the 233

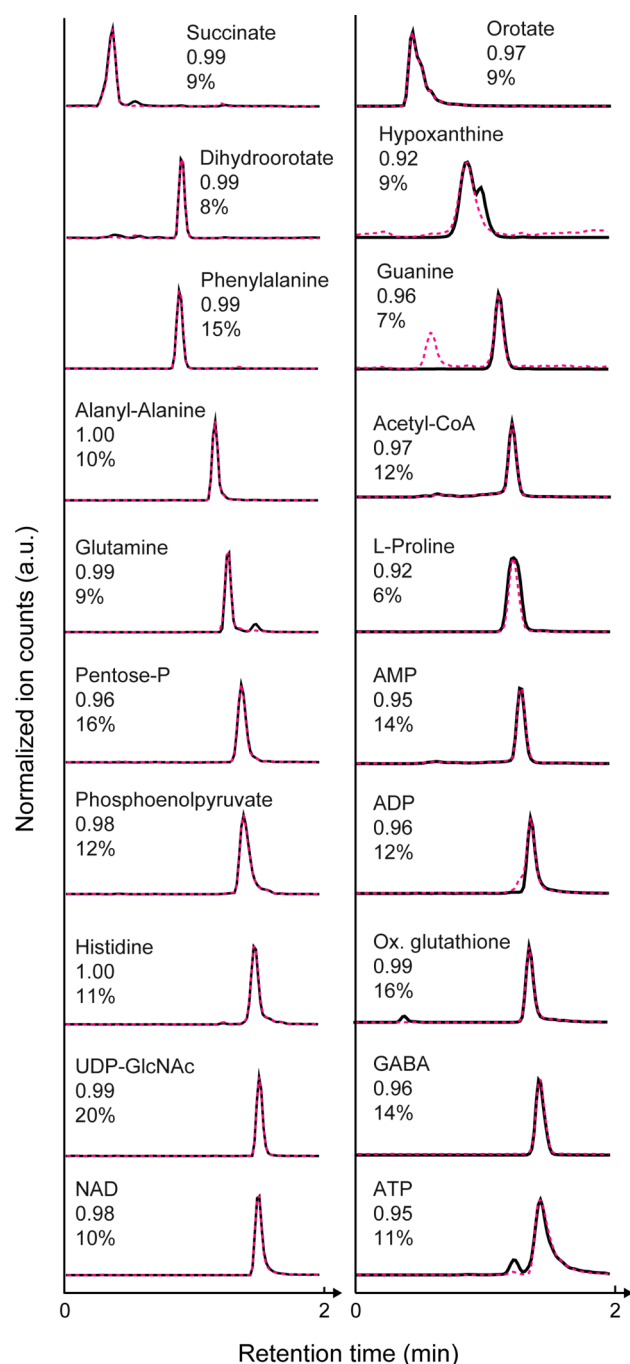


Figure 1. Time-optimized LC-MS/MS. Overlay of ^{12}C (black) and ^{13}C (magenta) chromatograms of 10 metabolites measured with Method A (left) and Method B (right). The correlation score and the RSD are given below to the name of a metabolite.

metabolites with a score >0.8 and $\text{RSD} < 20\%$, 141 resulted from MRMs obtained by single compound optimization or the literature. The remaining 92 metabolites were derived from predicted MRMs, and they included important analytes such as the purine nucleotide precursor 5-amino-1-(5-phospho-D-ribose)imidazole-4-carboxamide (AICAR).

Selectivity. To validate the selectivity of the methods, we spiked 79 authentic standards into a typical *E. coli* sample and measured MRMs for 180 out of the 233 high-scoring metabolites. This required three injections with method A and three injections with method B to enable sufficient dwell

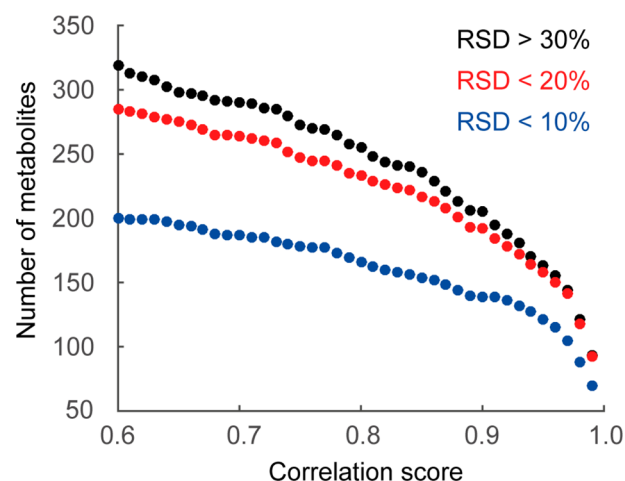


Figure 2. Testing MRM assays of 419 metabolites. Number of metabolites above the correlation-based score on the x-axis are shown for three relative standard deviations (RSD).

times of 10 ms. For each MRM, we calculated outliers to identify which of the 79 spiked samples was significantly changed (Figure S2 and Table S3). Selectivity of 86% of the MRMs for which we had standards was validated, as they only changed in samples spiked with the correct standards. As expected, the MRM assay $259 > 79$ detected the three samples spiked with glucose-6-P, fructose-6-P, and glucose-1-P (hexose-P), $229 > 79$ detected ribose-5-P, ribose-1-P, and ribulose-5-P (pentose-P), and $132 > 86$ detected leucine and isoleucine. Generally, the short LC-MS/MS methods were not able to separate these isomers and only quantify their pooled concentration. Also the MRMs for threonine and homoserine detected both metabolites. Lysine and glutamine were also detected by same MRMs and we reassigned lysine to Method A that separated these metabolites (Figure 3A). Only 5 MRMs did not detect the respective standard. For example, the MRM for ornithine falsely detected citrulline, due to the in-source fragmentation of citrulline into ornithine.¹⁴ We realized that only Method A achieves good separation of ornithine and citrulline (Figure 3B). The sample spiked with dihydroxyacetone-P (DHAP) was falsely detected by the MRM for fructose-1,6-PP (FBP). To exclude that residual enzymatic activity in the spiked sample converted DHAP into FBP, we analyzed a pure DHAP standard. The DHAP standard had again a signal in the FBP channel, which matched the peak in DHAP channel (Figure 3C). Because an FBP standard eluted later from the column, we assume that an aldol reaction in the ion source converts DHAP into FBP (Figure 3C). In-source fragmentation of nucleosides into nucleobases was not problematic, because they were sufficiently separated as exemplified for inosine and hypoxanthine (Figure 3D). We observed no oxidation of NADH into NAD^+ during ionization, and both metabolites were well separated by Method B (Figure 3E). However, small amounts of the NADH and NADPH standards were oxidized (Figure 3E). Similarly, little hydrolysis of nucleotide diphosphates standards resulted in spurious signals in the channel of the respective monophosphate. In case of the 106 MRMs for which we had no standards, 27 falsely detected one or more of the spiked samples. The MRM for dihydrouracil, for instance, detected the sample spiked with orotate and the retention time indicated in-source fragmentation of orotate. Whether the other false hits were caused by unspecific MRMs

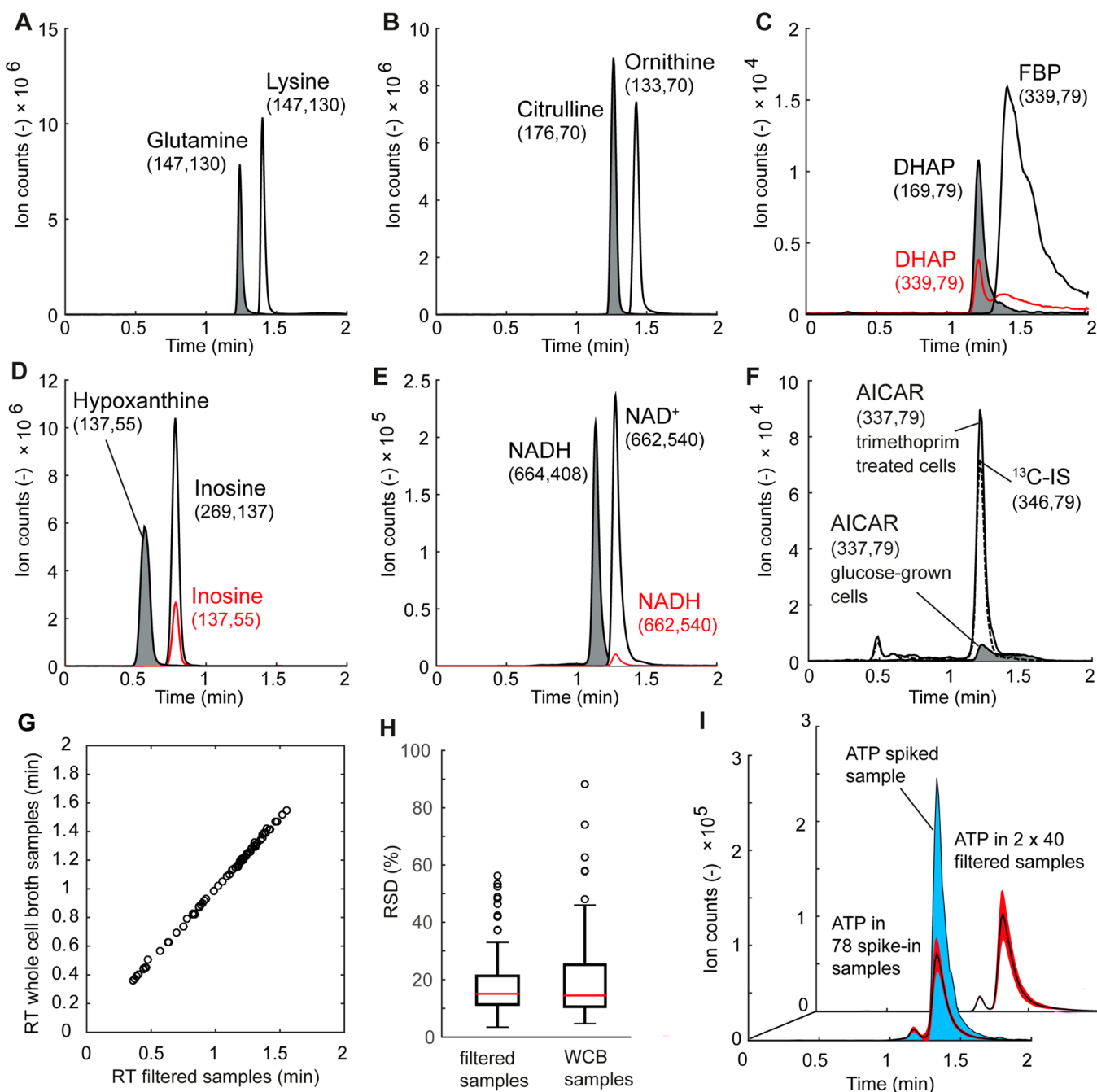


Figure 3. Method validation: (A) Chromatograms of lysine and glutamine standards ($1 \mu\text{M}$) with method A. MRMs used for detection of the respective compound are given in parentheses. (B) Chromatograms of ornithine and citrulline standards ($1 \mu\text{M}$) with method A. (C) Chromatograms of DHAP and FBP standards ($1 \mu\text{M}$) with method B. (D) Chromatograms of inosine and hypoxanthine standards ($1 \mu\text{M}$) with method A. (E) Chromatograms of NAD⁺ and NADH standards ($1 \mu\text{M}$) with method B. (F) Chromatograms of AICAR in samples of glucose-grown and trimethoprim treated cells with method B. (G) Comparison of retention times in filtered samples and in the sample of the whole culture broth. (H) RSD for 109 metabolites with score >0.8 in filtered samples and 87 metabolites in WCB samples. Boxes contain the middle of 50% of the data and whiskers indicate the 10th and 90th percentiles. (I) Chromatograms of ATP in the spike-in experiment and in 80 filtered samples measured in two independent batches on a column with >1000 injections. Black lines are the mean and red areas the standard deviation of the chromatograms. The chromatogram in blue was measured in the sample spiked with ATP.

or in-source fragmentation requires analyses of authentic standards for these compounds. Nevertheless, we attempted to test the selectivity of the MRM assay for AICAR without having an authentic standard.

Therefore, we indirectly inhibited the AICAR and folate consuming reaction in purine nucleotide biosynthesis by adding the folate biosynthesis inhibitor trimethoprim to glucose-grown

E. coli cells. Indeed, the signal for AICAR increased in trimethoprim treated cells, whereas it was almost not detectable in glucose-grown cells (Figure 3F).

In conclusion, the spike-in experiment validated selectivity of 64 MRMs and demonstrated the absence of unspecific responses for 79 MRMs. The remaining 37 MRMs were either

not selective or unspecific, and we excluded them from further analysis.

Robustness. To test how robust the methods are against variation of sample matrix, we measured all validated metabolites in a filtered *E. coli* metabolite extract and an extract from the whole culture broth (WCB). The latter contains a high amount of salt from the culture medium and is usually difficult to analyze by LC–MS/MS. A total of 120 samples were analyzed in three independent batches at three different days. In total, 80 samples of the first two batches were from the same filtered sample, and 40 samples of the third batch were from the WCB sample. In the filtrated samples, we detected 109 metabolites with a correlation based score >0.8 and in the WCB samples 87 metabolites. Retention times were the same in filtrated and WCB samples, demonstrating that the methods are robust against the high salt content of the WCB samples (Figure 3G). Moreover, retention times matched those in the spike-in experiment, showing long-term stability of the methods (Figure S3). The analytical results were consistent over the whole analysis, and the median RSD of $^{12}\text{C}/^{13}\text{C}$ ratios was 15% for the 80 filtered samples and 14% for the 40 WCB samples (Figure 3H). Peak shapes were also robust and did not change during the measurements. The only metabolites with noticeable peak shape variations were nucleotide triphosphates, as exemplified by the chromatogram of ATP (Figure 3I). However, to ensure stable peak shapes and retention times, it is important to inject 10 blanks (acetonitrile/methanol/water) before each batch.

Sensitivity and Linearity. Typical intracellular metabolite concentrations range between 1 μM and 10 mM^{25} and are usually 500 to 1000-fold diluted during sample processing (assuming no concentration step). Thus, the expected concentration range in the final sample is between 1 nM and 10 μM . To test if the fast LC–MS methods provide sufficient linearity and sensitivity in this range, we focused on the 64 metabolites for which we had standards and validated MRMs. We prepared a mixture of these metabolites at 10 different concentrations between 0.4 nM and 10 μM , spiked in ^{13}C -IS and measured the metabolites with a single injection on method A and a single injection on method B (Table S4). Only 3 metabolites had an $R^2 < 0.9$ (Figure 4), and these were hexose-P and citrate due to hyperbolic calibration curves. CDP did not correlate with the standard and was generally difficult to detect. All calibration curves were forced through the origin due to the assumption that $^{12}\text{C}/^{13}\text{C}$ -ratios are zero when no ^{12}C standard is present. In order to validate this assumption, we calculated calibration curves with a y -intercept and tested if the 99% confidence interval of the y -intercept includes zero (Table S4). Five of the 64 y -intercept confidence intervals did not include zero, and these were citrate, CDP, ATP, GTP, and aspartate. However, their y -intercept intervals missed the zero cutoff by less than 0.04, suggesting only small interferences in the lower concentration range of these metabolites (Table S4). On the basis of the calibration curves, we calculated concentrations of ^{13}C labeled metabolites in the ^{13}C -IS (Figure 4). Most metabolites lay within the range of 1 nM to 10 μM , matching the concentration range of final extracts that we expected initially. With 1 nM, inosine and guanosine showed the lowest concentration, while we measured the highest concentration for reduced glutathione and glutamate at 16 μM and 37 μM , respectively. On the basis of these results, we concluded that our methods provide sufficient linearity and

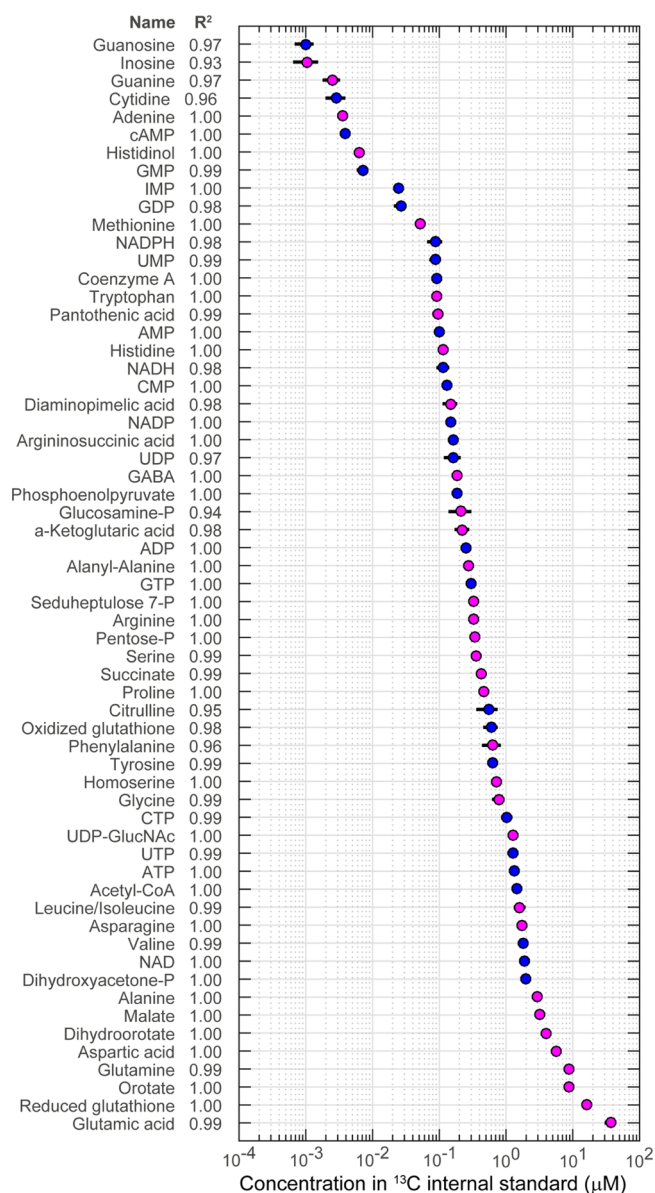


Figure 4. Absolute metabolite concentrations in the ^{13}C internal standard. Shown are concentrations of 61 metabolites with $R^2 > 0.9$. Colors indicate the LC–MS/MS method used for quantification (red, method A; blue, method B). Dots are concentrations that were estimated by a linear regression of calibration curves. Lines indicate 95% confidence intervals. The R^2 of the linear regression is given next to each metabolite.

sensitivity to quantify metabolites in cell extracts directly, and no concentration step is required.

Metabolite Concentrations in *E. coli*. Finally, we validated the quantitative performance of the LC–MS/MS methods. Therefore, we grew *E. coli* MG1655 on glucose minimal medium and collected three samples during midexponential growth. We measured the same metabolites that we already quantified in the ^{13}C -IS using again one injection with Method A and one with Method B (Table S4). The measured concentrations in glucose-grown MG1655 cells were remarkably consistent with previously reported concentrations of *E. coli* NCM3722 grown on glucose agarose-plates²⁵ (Figure 5). In both data sets, the most abundant metabolites are glutamate and glutathione, and the nucleosides cytidine and

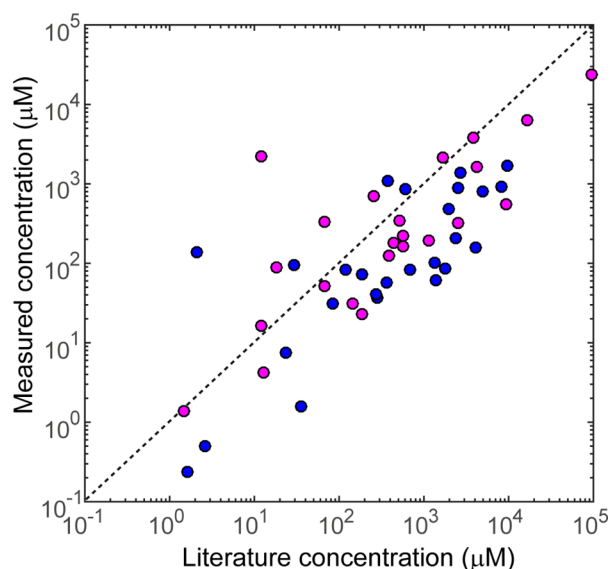


Figure 5. Absolute metabolite concentrations in *E. coli*. Measured metabolite concentrations in *E. coli* MG1655 are plotted against concentration reported in ref 25. Colors indicate method A (pink) and method B (blue).

guanosine have the lowest concentration. Additionally, the high adenylate energy charge of 0.93 (1.7 mM ATP, 0.2 mM ADP, and 0.04 mM AMP) in glucose-grown cells demonstrates that fast LC–MS/MS generates biologically meaningful metabolome data.

CONCLUSIONS

We demonstrated that fast LC–MS/MS analysis using 2 min runs provides a robust analytical strategy for quantitative high-throughput metabolomics. Short LC columns and optimized HILIC conditions were important for this development, especially since HILIC based chromatography enabled us to omit ion-pairing reagents and measure metabolites extracted in organic solvents. Reproducibility and linearity of time-optimized LC–MS/MS was comparable to methods using longer chromatographic runs,^{9,10} and a thorough spike-in experiment demonstrated the high selectivity. Robustness of the methods against salt enables analyses of samples from the whole culture broth, which are particularly important for high-throughput and automated sampling.⁴ The sensitivity in the range of 1 nM to 10 μ M allows direct measurements in nonconcentrated cell extracts and thereby strongly facilitates sample preparation. The combination of fast sample preparation and rapid measurements is especially important when the metabolites of interest are unstable or very reactive. Limitations of fast LC–MS/MS are that isomers are not sufficiently separated and that dwell times limit the number of compounds measured in a single run. From our experience, it is possible to measure between 30 and 40 metabolites with a single 2 min LC–MS/MS method. We expect that the new generation of QqQ instruments with even faster MRM assays will soon overcome this limitation, allowing quantification of >100 metabolites in a 2 min run. In summary, fast isotope ratio LC–MS/MS can quantify metabolites in 2 min and the targeted compounds can be selected from a database with 143 validated MRMs (Table S3) and 854 prescreened MRMs (Table S2).

ASSOCIATED CONTENT

Supporting Information

The Supporting Information is available free of charge on the ACS Publications website at DOI: 10.1021/acs.analchem.6b03731.

Algorithm for peak selection and scoring in Matlab format; Figure S1, differences between $^{12}\text{C}/^{13}\text{C}$ ratios determined with methods A and B; Figure S2, selectivity test for 79 single compounds against 180 MRMs; Figure S3, retention times in spike-in samples and filtered samples (PDF)

Table S1, RSDs of 40 metabolites measured with the 24 LC methods in Table 1; Table S2, 854 MRMs assays for 419 metabolites and their performance with methods A and B; Table S3, MRMs and results of 180 metabolites in the spike-in experiment; Table S4, calibration and absolute concentrations in *E. coli* MG1655 for 64 validated metabolites (XLSX)

AUTHOR INFORMATION

Corresponding Author

*E-mail: hannes.link@synmikro.mpi-marburg.mpg.de.

ORCID

Hannes Link: 0000-0002-6677-555X

Author Contributions

J.C.G. and T. Schramm contribute equally. J.C.G. cowrote the manuscript and performed experiments. T. Schramm performed experiments and cowrote the manuscript. T. Sander performed experiments. H.L. performed experiments, cowrote the manuscript, and directed the project.

Notes

The authors declare no competing financial interest.

ACKNOWLEDGMENTS

We thank J. M. Buescher, T. J. Erb, S.-M. Fendt, J. Plumbridge, and D. C. Sévin for discussions. This work was supported by Deutsche Forschungsgemeinschaft Grant LI 1993/2-1.

REFERENCES

- (1) Madalinski, G.; Godat, E.; Alves, S.; Lesage, D.; Genin, E.; Levi, P.; Labarre, J.; Tabet, J.-C.; Ezan, E.; Junot, C. *Anal. Chem.* **2008**, *80*, 3291–3303.
- (2) Beckmann, M.; Parker, D.; Enot, D. P.; Duval, E.; Draper, J. *Nat. Protoc.* **2008**, *3*, 486–504.
- (3) Fuhrer, T.; Heer, D.; Begemann, B.; Zamboni, N. *Anal. Chem.* **2011**, *83*, 7074–7080.
- (4) Link, H.; Fuhrer, T.; Gerosa, L.; Zamboni, N.; Sauer, U. *Nat. Methods* **2015**, *12*, 1091–1097.
- (5) Cajka, T.; Fiehn, O. *Anal. Chem.* **2016**, *88*, 524–545.
- (6) Grüning, N. M.; Rinnerthaler, M.; Bluemlein, K.; et al. *Cell Metab.* **2011**, *14*, 415–427.
- (7) Taymaz-Nikerel, H.; De Mey, M.; Baart, G. J. E.; et al. *Biotechnol. Bioeng.* **2016**, *113*, 817–829.
- (8) van Eunen, K.; Kiewiet, J. A. L.; Westerhoff, H. V.; Bakker, B. M. *PLoS Comput. Biol.* **2012**, *8*, e1002483.
- (9) McCloskey, D.; Gangotti, J. A.; Palsson, B. O.; Feist, A. M. *Metabolomics* **2015**, *11*, 1338–1350.
- (10) Bajad, S. U.; Lu, W.; Kimball, E. H.; Yuan, J.; Peterson, C.; Rabinowitz, J. D. *J. Chromatogr. A* **2006**, *1125*, 76–88.
- (11) Buescher, J. M.; Moco, S.; Zamboni, N. *Anal. Chem.* **2010**, *82*, 4403–4412.
- (12) Bennett, B. D.; Yuan, J.; Kimball, E. H.; Rabinowitz, J. D. *Nat. Protoc.* **2008**, *3*, 1299–1311.

- (13) Wu, L.; Mashego, M. R.; van Dam, J. C.; et al. *Anal. Biochem.* **2005**, *336*, 164–171.
- (14) Xu, Y.-F.; Lu, W.; Rabinowitz, J. D. *Anal. Chem.* **2015**, *87*, 2273–2281.
- (15) Creek, D. J.; Jankevics, A.; Breitling, R.; Watson, D. G.; Barrett, M. P.; Burgess, K. E. V. *Anal. Chem.* **2011**, *83*, 8703–8710.
- (16) Zhang, T.; Creek, D. J.; Barrett, M. P.; Blackburn, G.; Watson, D. G. *Anal. Chem.* **2012**, *84*, 1994–2001.
- (17) Callahan, D. L.; De Souza, D.; Bacic, A.; Roessner, U. *J. Sep. Sci.* **2009**, *32*, 2273–2280.
- (18) Zhang, R.; Watson, D. G.; Wang, L.; Westrop, G. D.; Coombs, G. H.; Zhang, T. *J. Chromatogr. A* **2014**, *1362*, 168–179.
- (19) Kim, S. H.; Yoo, H. H.; Cha, E. J.; et al. *Mass Spectrom. Lett.* **2013**, *4*, 47–50.
- (20) Dunn-Meynell, K. W.; Wainhaus, S.; Korfmacher, W. A. *Rapid Commun. Mass Spectrom.* **2005**, *19*, 2905–2910.
- (21) Zhang, A.; Sun, H.; Han, Y.; et al. *Anal. Chem.* **2013**, *85*, 7606–7612.
- (22) Fuhrer, T.; Zamboni, N. *Curr. Opin. Biotechnol.* **2015**, *31*, 73–78.
- (23) Chambers, M. C.; Maclean, B.; Burke, R.; et al. *Nat. Biotechnol.* **2012**, *30*, 918–920.
- (24) Allen, F.; Pon, A.; Wilson, M.; Greiner, R.; Wishart, D. *Nucleic Acids Res.* **2014**, *42*, W94–W99.
- (25) Bennett, B. D.; Kimball, E. H.; Gao, M.; Osterhout, R.; Van Dien, S. J.; Rabinowitz, J. D. *Nat. Chem. Biol.* **2009**, *5*, 593–599.